Research on Microchannel Flow Field and Filtration Characteristics of Two-dimensional Fiber Layer

Jingming Li[1, a], Zhaodong Huang[2, b], Jiahui Xu[3, c], Yadi Wang[4, d]

[1] School of New Energy, Xi'an Shiyou University, Xi'an 710043, China

[2] School of Mechanical Engineering, Xi'an Shiyou University, Xi'an 710043, China

[3] School of Mechanical Engineering, Xi'an Shiyou University, Xi'an 710043, China

[4] School of Mechanical Engineering, Xi'an Shiyou University, Xi'an 710043, China

[a]lijm@xsyu.edu.cn, [b]huangzhaodong1255@163.com, [c]xujiahui0226@163.com, [d]wangyadi0605@163.com

Abstract

In the multi-scale study of fiber filtration mechanism, this study investigates the regulation mechanism of aerosol deposition behavior by shaped fiber layers through numerical simulation system. A two-dimensional model is constructed for circular fiber layer, square fiber layer, and r=1, 2, 3 curved angular fiber layer. Based on the transient gas-solid coupling algorithm, we analyze the dynamic deposition process of particles under unsteady conditions, focus on the synergistic effects of Brownian diffusion, inertial collision, and interception effect in the transport of particles with multiple particle sizes, and analyze the effects of these factors on the deposition of particles on fibers and the performance of fiber trapping. The study reveals that as the competitive relationship between Brownian diffusion and inertial collision to achieve an optimal balance of capture efficiency and pressure loss in submicron particle filtration - sharp corners (e.g., square, r=1) enhance local turbulence and diffusive interception at the expense of flow field stability, while smooth curvature (e.g., round, r=3) suppresses separation eddies, reduces energy consumption, but weakens the diffusion effect - needs to be A compromise curvature (e.g., r=2) is chosen based on the target particle size (R-value) and flow velocity to synergize the inertia-diffusion capture path.

Keywords

Microchannel Filtration; Fiber Structure; Particle Characterization; Simulation.

1. Introduction

As the national economy continues to soar and the quality of life in society steadily improves, people's needs are gradually shifting from the basic material level to the higher level of spiritual and cultural fields, and it is more important than ever to ensure a healthy and safe living environment for people. Relevant studies have shown that there are significant differences in the degree of harm to human health caused by particles of different sizes in the air, and that the morbidity and mortality rates of people who have been exposed to excessive pollution for a long period of time have shown a significant increase. In terms of the composition of pollution sources, pollutants generated by anthropogenic activities dominate. Mineral dust, coal combustion dust and carbon-based particulate matter generated during industrial production, automobile exhaust, chemical vapors, and forest fire smoke together constitute the major sources of air pollution. In addition, in the natural formation of biological suspended matter, plant pollen, pathogenic microorganisms and virus carrier aerosols, when encountered with specific climatic conditions so that still back to the human body to produce health threats. Among the air pollutants that affect human life and health, fine particulate matter (PM) is the most hazardous [1]. In the precision manufacturing process, the accumulation of pollutants on the surface of the substrate directly affects the process yield and product performance stability. Take optical components as an example, the presence of micron-sized foreign matter adhering to its transparent interface will trigger the phenomenon of light wave transmittance attenuation, and this nonlinear optical loss is particularly significant in the coating layer of photolithography equipment lenses or display panels, and particle deposition on the surface of the photoreceptor will lead to signal distortion. In the operating room, intensive care unit and coronary care unit and other medical places, particle contamination will lead to the cleanliness level of these places is reduced, prone to cause wound pathogenic bacteria infection, with adverse consequences [5].

A number of scholars have investigated the filtration performance of square cross-section fibers using theoretical analysis and numerical simulation methods, such as Fardi and Liu [6] who took the lead in quantifying the correlation law of aspect ratio on pressure drop and diffusion capture using a coupled multi-physics-field model, revealing that the cross-sectional aspect ratio affects the efficiency threshold by altering the location of the separation point of the bypassing flow, and thus, Zhu [7] proposed the efficiency prediction formula for the inertia-interception dual mechanism , as well as proposed the influence of factors such as cross-section aspect ratio and Stokes number on the filtration performance. And based on the numerical analysis, the formula for the fiber capture efficiency under two mechanisms was proposed. And based on this, rectangular hydraulic diameter was introduced to analyze the effect of particle size distribution on particle deposition performance by numerical calculation. For the prismatic effect, Fardi and Benjamin [8] carried out the corresponding flow analysis for the prismatic angle of square fibers, and analyzed that the sharp-angled structure of the channel is prone to inducing the secondary flow, which leads to the increase of the local pressure loss but the probability of collision has been improved compared with the previous one. However, it is not suggested how the angular angle can be changed to achieve a better flow condition.

Huang [9] numerically simulated the particle capture process for submicron particles and investigated the effect of four shaped cross-section shapes (trilobal, rectangular, and quadrilobal) of fibers on their capture performance, and found that the shaped cross-section was better for their capture performance and the particles of the fibers in the elliptical shape were more uniformly distributed, and finally, the structure of dendritic clusters was formed. Sekiguchi et al [10], in order to accurately predict the coarse and fine fiber composite efficiency model, an empirical formula for filtration efficiency was developed considering the diameter and weight of coarse and fine fibers.Chen [11] numerically simulated the deposition characteristics of non-spherical particles by using four different simulation methods such as CFD-DPM, CFD-DEM, loaded resistance model based on the API interface of EDEM software and EDEM simulation.

In order to solve these problems, this study investigates the regulation mechanism of aerosol deposition behavior by shaped fiber layers through a numerical simulation system. A two-dimensional model is constructed for circular fiber layer, square fiber layer, and r=1, 2, 3 curved angular fiber layer. Based on the transient gas-solid coupling algorithm, we analyze the dynamic deposition process of particles under unsteady conditions, focus on the synergistic effects of Brownian diffusion, inertial collision, and interception effect in the transport of particles with multiple particle sizes, and analyze the effects of these factors on the deposition of particles on fibers and the performance of fiber trapping.

2. Mathematical Modeling Approach

2.1 Fluid Governing Equations

(1) Mass Conservation Equation

In the numerical modeling of fiber filtration systems, the law of conservation of mass serves as the central physical constraint to strictly characterize the dynamic equilibrium of the flowing medium through the integral form of the continuity equation. Based on the discrete framework of the finite volume method, the mass flux of the fluid phase in each computational unit is coupled with the particle deposition effect to form a conservation characterization system of the aerosol transport and retention process in the porous medium, which lays the theoretical foundation for revealing the intrinsic correlation between the filtration efficiency and the evolution of the flow field. The mass conservation equations are calculated as follows:

$$\frac{\partial\rho}{\partial t}+\frac{\partial(\rho u)}{\partial x}+\frac{\partial(\rho v)}{\partial y}+\frac{\partial(\rho w)}{\partial z}=0 \tag{1}$$

Where t is the time, s;ρ is the fluid density, kg/m^3;u is the velocity vector component in the x-direction, m/s;v is the velocity vector component in the y-direction, m/s;w is the velocity vector component in z direction, m/s.

(2) Conservation Of Momentum Equation

The law of conservation of momentum, which is a law that must be satisfied in all flow problems, can be expressed as follows: the rate of increase of the fluid flow in a micrometric body is equal to the sum of the various forces acting on the micrometric body.

$$\frac{\partial(\rho u)}{\partial t}+div(\rho uu)=-\frac{\partial p}{\partial x}+\frac{\partial\tau_{xx}}{\partial x}+\frac{\partial\tau_{yx}}{\partial y}+\frac{\partial\tau_{zx}}{\partial z}+F_x \tag{2}$$

$$\frac{\partial(\rho v)}{\partial t}+div(\rho vu)=-\frac{\partial p}{\partial x}+\frac{\partial\tau_{xy}}{\partial x}+\frac{\partial\tau_{yy}}{\partial y}+\frac{\partial\tau_{zy}}{\partial z}+F_y \tag{3}$$

$$\frac{\partial(\rho w)}{\partial t}+div(\rho wu)=-\frac{\partial p}{\partial x}+\frac{\partial\tau_{xz}}{\partial x}+\frac{\partial\tau_{yz}}{\partial y}+\frac{\partial\tau_{zz}}{\partial z}+F_z \tag{4}$$

Where τ p is the pressure on the fluid microelement, Pa;τ_{xx} is the surface viscous stress component of the xx surface-acting microelement, N/m^2;τ_{yy} is the surface viscous stress component of the yy surface-acting microelement, N/m^2;τ_{zz} is the surface viscous stress component of the microelement body acting on the zz-plane, N/m^2; F_x is the component force in the x-direction, N.

(3) Particle Phase

The equations of translation and rotation of particle i are as follows:

$$\frac{dx_i}{dt}=v_{ix} \tag{5}$$

$$M_i\frac{dx_i}{dt}=\sum_i\left(F_{n.ij}+F_{t.ij}\right)+F_{g.j}+F_{v.ij}+m_ig \tag{6}$$

$$I_i\frac{d\omega_i}{dt}=\sum_j T_{ij} \tag{7}$$

$$I_i = \frac{2}{5} m r_i^2 \tag{8}$$

Where:x_i is the particle position, m;v_i is the particle velocity, m/s;m_i is the particle mass, kg. $F_{n.ij}$ is the normal contact force, N; $F_{t.ij}$ is tangential contact force, N; $F_{g.j}$ is the fluid force on the particle, N; $F_{v.ij}$ is the van der Waals force, N; g is the gravitational acceleration, m/s^2; I_i is the particle rotational inertia, kg-m^2; ω_i is the particle angular velocity, rad/s; $T_{i.j}$ is the torque, N-m; r_i is the particle radius, m.

3. Physical Modeling and Parameterization

In this study, a two-dimensional fiber microchannel model was constructed. In the 2D model, the inlet and outlet of the microchannel are open. In order to overcome the effect of uneven distribution of inlet flow velocity, an inlet channel with a length of 25 cm was introduced in the original model. In addition, all other conditions were the same for the five models.

Table 1. Geometry of different fiber models

Mould	L_1(μm)	L_2(μm)	L_3(μm)	L_4(μm)
Circular	80	10	25	12
Square	80	10	25	20
r=1	80	10	25	16
r=2	80	10	25	16
r=3	80	10	25	16

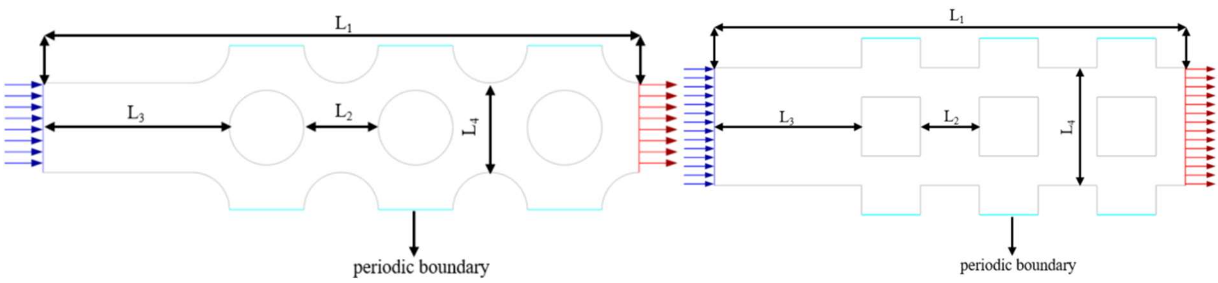

(a)Circular fiber layer (b)Square fiber layer

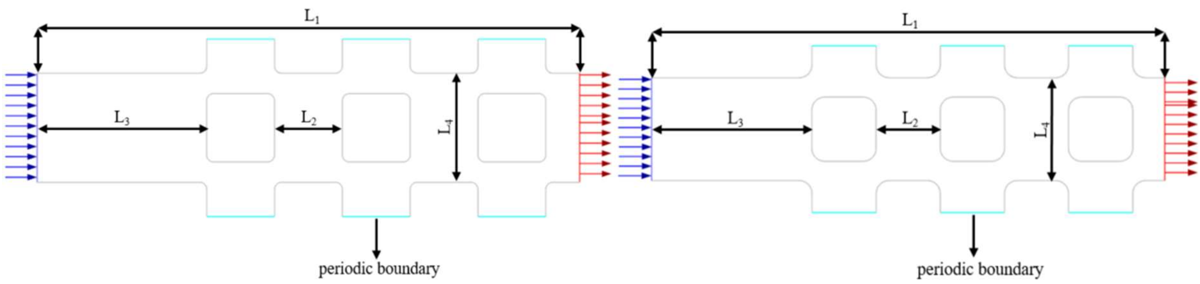

(c)r=1 fiber layer (d)r=2 fiber layer

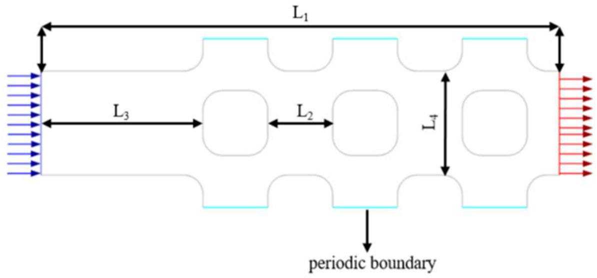

(e)r=3 fiber layer

Figure 1. Geometry of different fiber models

In the high-precision numerical simulation of the fiber-winding flow field, Fluent double-precision solver is used to construct the computational framework, and the pressure-velocity field is efficiently coupled with SIMPLEC algorithm through the second-order windward format of the discrete control equations, and the convergence residual threshold is set to 10-9 to ensure the computational accuracy. The computational domain adopts a structured advective grid system, and the fiber near the wall is encrypted by a two-layer boundary layer, and the physical scenario of infinite fiber array is simulated by the periodic boundary conditions - the particle escape and injection at the upper and lower boundaries follow the real fiber arrangement law. The numerically solved boundary conditions are: velocity inlet and pressure outlet for the basin inlet and outlet, respectively; the fiber wall is set as a no-slip boundary; and the upper and lower boundaries of the computational domain are periodic boundaries.

4. Results and Discussion

In the Brownian diffusion-dominated filtration of small particles of 0.01 μm <dp< 0.2 μm, Figure 1-1(a) demonstrates the correlation law between the capture efficiency of the square fiber layer and the Péclet number (Pe), which characterizes the relative importance of the advective transport versus diffusive action in the particle motion. For very small particles (dp=0.01 μm, Pe=410), Brownian diffusion dominates and the particles frequently collide with the fiber surface due to stochastic thermal motion, and the capture efficiency is high. At this time, the influence of the trailing force on the particle trajectory is weak, and the migration path of the particles is mainly controlled by the disordered Brownian motion. However, as the particle size increases (dp=0.2 μm, Pe=8204), the Brownian force attenuates significantly, the advective transport effect is enhanced, and the tendency of the particles to move along the streamline is strengthened, resulting in a lower probability of collision with the fiber surface and a sudden drop in the capture efficiency. This phenomenon indicates that when Pe>1000, the diffusion mechanism still dominates the capture process, but its effectiveness has been limited by the enhanced particle inertia. Figure 1-1(b) further reveals the dynamic characteristics of particle distribution at high Pe number (Pe=8204). The irregular spatial distribution of the particles at t=0.005 s indicates that their motion is subject to the combined effect of diffusion and advection. On the one hand, the residual Brownian force causes the particle trajectory to deviate from the main flow line; on the other hand, the airflow trailing force pushes the particles to migrate along the direction of the flow field. This mixing mechanism leads to the formation of a sparse collision distribution of particles near the fiber surface instead of uniform deposition. It can also be seen that some of the particles in the flow field to form a “roundabout” trajectory, only in the corners of the fiber and other local high shear region of the short stay, further reducing the effective capture probability. The geometric properties of the square fiber layer exacerbate the flow separation at the corners to generate vortices, which perturb the direction of particle motion, making it easier for particles to detach from the fiber surface, especially at high flow velocities. The effect of fiber geometry is more prominent at high Pe-numbers, and the corners of square fibers enhance the local shear effect, but also reduce the particle residence time through flow separation, which is a contradiction that needs to be balanced by optimizing the fiber corners (e.g., by using a curved-corner

 Volume 11 Issue 6, 2025
DOI: 10.6919/ICJE.202506_11(6).0009

design). Overall, the design of filtration systems for submicron particles requires a synergistic matching mechanism between fiber geometry, flow rate control, and particle size distribution to maximize the capture efficiency in the diffusion-dominated region.

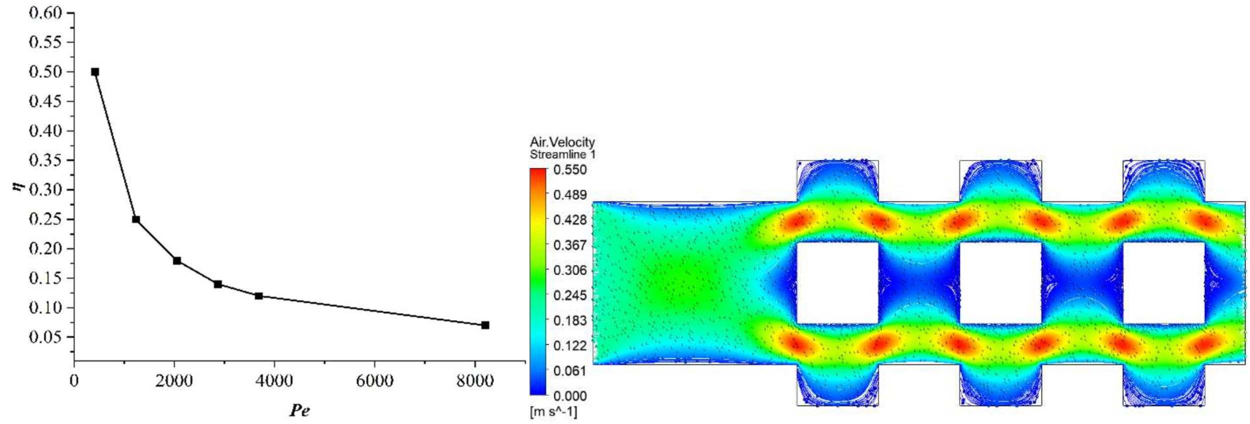

(a) (b)

Figure 2. (a) Capture efficiency of square fiber layer in the Brownian diffusion dominated case; (b) Particle distribution at Pe=8204, t=0.005s

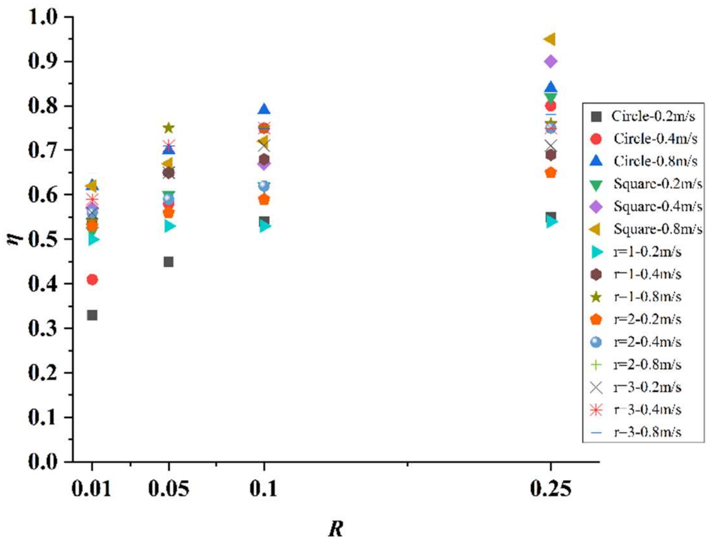

Figure 3. Relationship between capture efficiency and R for circle, square, and three different fiber layer models with varying r.

In the study of fiber filtration mechanism, the physical nature of the geometric interception efficiency R is embodied as the size-matching effect of particles and fibers, and its quantitative parameter is the ratio of particle diameter to the characteristic scale of fibers. Figs. 1-2 reveal the correlation law between the capture efficiency and interception coefficient of the five shaped fiber models under different flow rate conditions. It can be seen in the figures that the fiber capture efficiencies of all five models increase with the increase of R, which ranges from 0.01 to 0.5. The results show that the capture characteristics of fibers with different geometrical shapes present significant differences when the R value changes, circular fibers show smooth efficiencies at low R values due to the homogeneity of the symmetric flow field, but their inertial collision efficiencies tend to saturate in the increase of the R value due to the limitation of the flow field characteristics, and the square fibers show significant differences in their capture characteristics when the R value varies. At medium R-value, the trapping efficiency increases rapidly due to the high shear effect at the corners, but at high R-value the violent flow separation leads to the secondary escape of particles, and the increase in efficiency is limited. In the curved fiber, the curved radius (r=1) enhances the local inertial collision through the sharp leading edge, which improves the efficiency significantly at low R-value, but the efficiency falls back due to the flow instability at high R-value; the curved radius (r=2) fiber balances the inertial collision and diffusive deposition effect in a wide range of R-value through the gentle geometrical transition, which forms the stable and efficient trapping interval; the design of curved radius (r=3) suppresses the separation intensity through the flow guidance effect and shows better pressure loss control at high R-values, but sacrifices some of the low R-value efficiency.

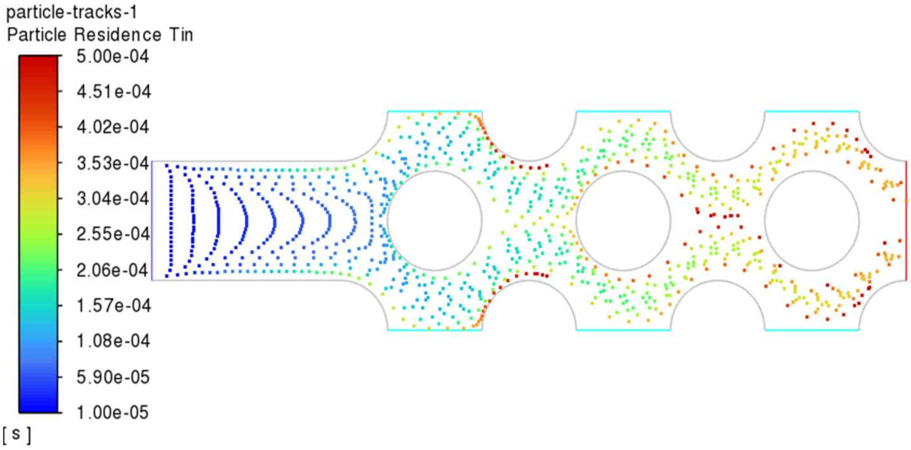

(a) Circular fiber layer

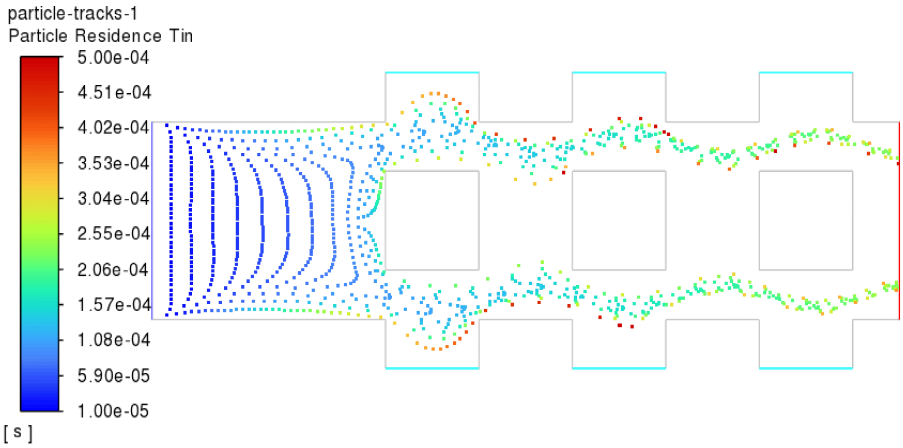

(b) Square fiber layer

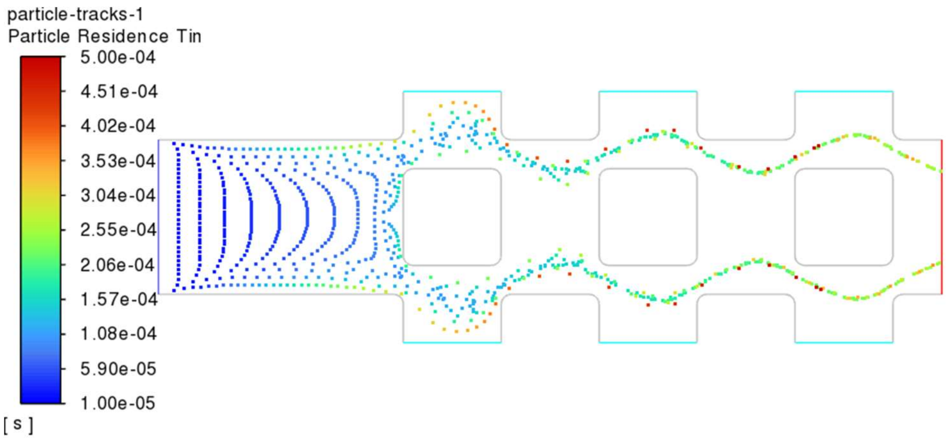

(c) r=1 fiber layer

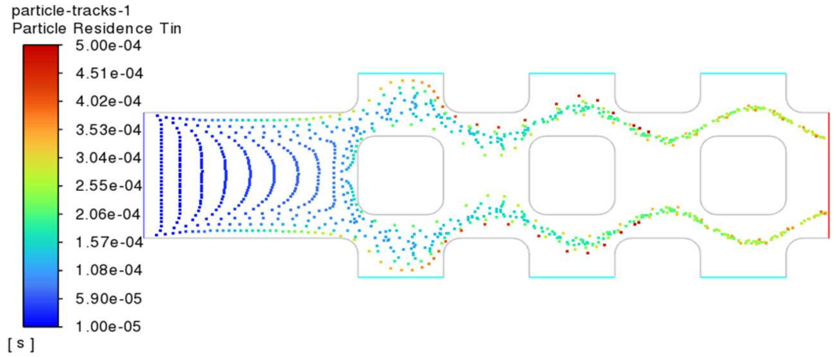

(d) r=2 fiber layer

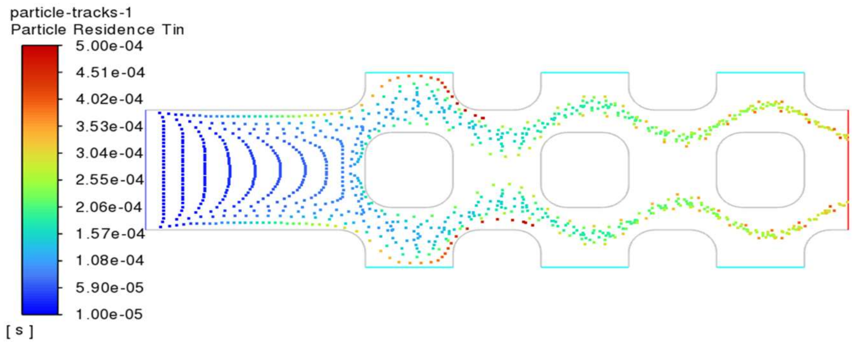

(e) r=3 fiber layer

Figure 4. Particle distribution of five fiber layer models at R=0.1 and t=0.0005s

Figures 4 demonstrate the particle distribution of the five fiber layer models at R = 0.1 and t = 0.0005 s. The distribution of particles at R = 0.1 and t = 0.0005 s is shown in Figures 1-3. From Figs. 1-3, it can be seen that the retention efficacy of all the five types of fiber configurations is significantly and positively correlated with the interception coefficient R. The staggered fiber arrays guide the aerosol particles to preferentially undergo collision adsorption in the windward region through the flow channel constriction effect, and although some particles can traverse the first fiber gap, the subsequent fiber arrangement will also capture the particles. In the circular fiber layer (a), the particle residence time distribution shows a uniform gradient, and the smoothness of the flow field makes the particles migrate along the main flow direction without significant perturbation, and only slight retention is formed on the leeward side of the fibers, which indicates that inertial collision is the dominant mechanism. The square fiber layer (b) with right-angled corners triggers the flow channel contraction effect, leading to the formation of a local high residence time band in the angular region, and the vortex separation phenomenon causes small particles to form a secondary adsorption layer behind the corners, which enhances the diffusion-interception coupling effect. r=1 curved angular cross-section layer (c) with sharp arcs leads to a significant distortion of the flow field, which prolongs the residence time of particles in the vicinity of the angular edges, and the Brownian diffusion paths are prolonged by the micro-vortices in the wake region, which improves particle trapping efficiency. path, and particle capture efficiency is improved. r=2 curved prismatic fiber layer (d) medium arc shape balances the flow field stability and separation effect, and the peak residence time in the main prismatic zone is reduced compared with r=1, but the secondary arc zone forms graded vortices, which optimizes the diffusion deposition efficiency of particles in the interstitial space of the fibers. r=3 curved prismatic fiber layer (e) close to the circular arc features make the residence time distribution close to that of the circular fiber layer (a), but in the residual prismatic layer (c) the residence time distribution of particles in the residual prismatic fiber layer is reduced.), but localized retention still exists in the residual angular region, suggesting the potential of the geometric transition morphology to modulate the inertia-diffusion synergy of submicron particles.

Overall, the curved structure of the fiber corners directly affects the complexity of the particle transport path and residence time distribution by modulating the flow field separation strength and vortex scale. Sharp angles (r=1) enhance diffusive interception efficiency through enhanced turbulence perturbation, while smooth curvature (r=3) optimizes the energy efficiency balance by reducing pressure drop, providing a quantitative basis for multi-objective filter material design.

5. Conclusion

In this study, the flow characteristics of particles within a fiber layer composed of different fiber shapes were investigated through a comprehensive simulation of a two-dimensional fiber layer. Subsequently, the effect of particle size on the 2D fiber layer pattern under various filter media conditions was systematically analyzed, and the following main conclusions were drawn:

a) Péclet number (Pe) is the core control parameter, reflecting the relative importance of convective transport and diffusion. Low Pe (Pe=410, dp=0.01μm): Brownian diffusion dominates, particles frequently collide with the fiber surface due to thermal movement, and the trapping efficiency is high. High Pe (Pe=8204, dp=0.2μm): inertia effect is enhanced, particles tend to migrate along the streamline significantly, and diffusion is limited resulting in a sudden drop in efficiency. The geometric effect of square fibers, the sharp corner area triggers flow separation and vortex, which disturbs the particle trajectory, shortens the retention time, and reduces the probability of effective capture. Optimization of corner curvature (e.g., rounding) is needed to balance shear enhancement with flow stability.

b) The symmetric flow field of circular fibers smooths the low R-value efficiency, but saturates the inertial collision efficiency at high R. The high shear effect at the corners of square fibers enhances the medium R-value efficiency, but the flow separation at high R leads to the secondary escape of particles. Curved fibers (r=1,2,3): small curvature (r=1): sharp leading edge enhances inertial collision, high efficiency at low R, but destabilization of the flow field at high R leads to a fallback in efficiency. Medium curvature (r=2): geometric gradient balances inertial collision and diffusive deposition, forming a stable and efficient region with wide R range. Large arc (r=3): close to circular features, inhibit flow separation, optimize pressure loss but sacrifice part of the low R efficiency.

c) Round fiber flow field is smooth, particles migrate along the main flow line, only slight retention on the leeward side, inertial collision dominated. Square fiber corner flow channel constriction to form a high retention zone, vortex generated secondary adsorption layer, coupled diffusion-interception effect. r=1 curved fiber micro-vortex to extend the diffusion path, enhance the corner zone capture efficiency. r=2 curved fiber graded vortex to optimize the fiber interstitial diffusive deposition. r=3 curved fiber close to the circular flow field characteristics, the residual corner zone retains the ability to retain the local retention.

Acknowledgments

Thank you to my family and teachers for their support.

References

[1] Chan C K, Yao X H. Air pollution in mega cities in China. Atmospheric Environment, 2008, 42:1–42.

[2] Li Z Q, Eck T, Zhang Y, et al. Observations of residual submicron fine aerosol particles related to cloud and fog processing during a major pollution event in Beijing [J]. Atmospheric Environment, 2014, 86: 187–192.

[3] Polichetti G, Cocco S, Spinali A, et al. Effects of particulate matter (PM10, PM2.5 and PM1) on the cardiovascular system [J]. Toxicology, 2009, 261(1-2): 1–8.

[4] Chang Y. China needs a tighter PM2.5 limit and a change in priorities. Environment Science and Technology, 2012, 46 (13): 7069–7070.

[5] Reinhardt K A, Kern W. Handbook of silicon wafer cleaning technology [M]. 3rd Edition. Oxford/Cambridge: William Andrew, 2018.

[6] Fardi B, Liu B Y. Flow field and pressure drop of filters with rectangular fibers [J]. Aerosol Science and Technology, 1992, 17(1): 36−44.

[7] Zhu C, Lin C H, Cheung C S. Inertial impaction-dominated fibrous filtration with rectangular or cylindrical fibers. Powder Technology, 2000, 112(1): 149-162.

[8] Fardi B , Liu B Y H .Efficiency of Fibrous Filters with Rectangular Fibers[J]. Aerosol Science & Technology, 1992, 17(1): 45-58.

[9] HUANG H, WANG K, ZHAO H. Numerical study of pressure drop and diffusional collection efficiency of several typical noncircular fibers in filtration[J]. Powder Technology, 2016, 292: 232-241.

[10] Sekiguchi, Y., Toyama, R. & Zama, Y. Estimation for Filtering Efficiency of Air Filter Consisting of Coarse and Fine Fibers. Aerosol Sci Eng 7, 325–340 (2023).

[11] Chen, L., Yuan, K., Qian, F.et al. Numerical investigation of non-spherical particle deposition characteristics on filter media. Build. Simul.16, 1331–1343 (2023).